Kinetics of Sorption of 1,3 Di-Isopropyl Benzene and 1,3,5 Tri-Isopropyl Benzene in Nay Crystals, Alumina Matrix and FCC Catalyst Particles by Zero Length Column Method

Kevin F. Loughlin, Sulaiman S. Al-Khattaf, and Sharif F. Zaman, King Fahd University of Petroleum & Minerals, P.O. Box 5050, Dhahran 31261, Saudi Arabia. Presented in Session: Fundamentals of Adsorption and Ion Exchange II (02E02), AIChE National Meeting, Cincinnati, Ohio, Oct. 30th – Nov. 4th 2005.

Abstract: The kinetics of sorption of 1,3 di-isopropyl benzene and 1,3,5 tri isopropyl benzene in NaY crystals, alumina matrix particles and FCC catalyst particles is reported. Both molecules were found to have highly nonlinear equilibrium adsorption properties in all three adsorbents and the observed K values are approximately 10^5. In NaY crystals, the desorption curve of 1,3 di-isopropyl benzene was normal, but that for 1,3,5 tri-isopropyl benzene contained a discontinuity reminiscent of a percolation threshold. The diffusivities in NaY crystals were micropore controlled and were determined from the nonlinear asymptotic form of the ZLC model. The alumina matrix particles, scanned by SEM to determine their size distribution, were macropore controlled in agreement with theory for 1,3,5 tri-isopropyl benzene. The FCC catalyst which is composed of 80 % alumina matrix and 20 % NaY crystals results are intriguing. The short term desorption appears macropore controlled. The long term diffusion asymptotes are identical for both sorbates to that for NaY crystals indicating micropore control but are significantly displaced due to the adsorption on the alumina matrix.

Introduction:

In FCC catalysts composed of a matrix alumina and embedded zeolites, the objective is to crack large bulky molecules of heavy oil into smaller molecules. Zeolite crystals of the faujasite type have small pore opening and don't permit large molecules to penetrate inside the zeolite cage. The outer surface of zeolite, which is only 3% of the total active site, is available for the larger molecules. Therefore zeolites are commonly combined with an amorphous matrix that cracks the larger molecules into smaller ones, which are then able to access the micropore system. Alumina is commonly used as a catalyst binder for FCC pellets. It has large mesopores and allows the larger molecules to penetrate inside the pellet to reach the micropore system. Diffusivity of large molecule through this mesopore/micropore system is important to understand the cracking mechanism of larger molecules in FCC catalysts.

Studies of the diffusion of large molecules in faujasite type materials, such as X or Y zeolite are reported by Satterfield and coworkers [Satterfield and Katzer [1], Moore and Katzer[2]], Moore[3] , Culfaz and Ergun[4], Ruthven and Kaul[5], Fujikata et al.[6], Hashimoto et al.[7], and Cavalcante et al.[8] among others. Moore[3] stated that the effective diffusion coefficient of the compact molecules [toluene, p xylene, naphthalene, 1-methylnaphthalene, 1-ethylnaphthalene, 2-ethylnaphthalene, and mesitylene] correlates with the diameter of the smallest orifice through which the molecule can pass (the critical diameter), decreasing as the critical diameter increases. But aromatic molecules with longer side chains, such as m-di iso-propylbenzene, or 1,3,5 triethylbenzene deviate from this correlation, perhaps because their structure is more easily deformed. Further, such molecules, with a critical diameter of 9.4 Å readily diffuse in the pore structure with an orifice diameter of 7.4 Å, although slowly. Ruthven and Kaul[5] report the diffusion of a range of aromatics [1,3,5 trimethylbenzene (mesitylene), 1,2,3,5 tetramethylbenzene, hexamethylbenzene, anthracene, and 1,3,5 triethylbenzene] in NaX zeolite. They confirm the validity of the diffusion model for several of the sorbates and successfully correlated their diffusivity data with the moment of inertia of the sorbate molecule with one exception. The specter of catalytic activity perturbs the measurement of diffusivities of large molecules. Ruthven and Kaul[5] used an inactive sodium form of zeolite X but even still suggested, that in contact with the zeolite, triethylbenzene is slowly reacting. The literature is replete with references of catalytic cracking and coke formation for 1,3,5 tri iso-propylbenzene [S-Aguir et al[9] & Al-Khattaf et al.[10])].

There are surprisingly few papers on the diffusion of large molecules in the gaseous phase in alumina but quite a lot on diffusion of liquids due to the interest on the ingress of asphaltenic molecules into the FCC catalyst structure via the alumina pathway. This topic is known as "Restrictive Diffusion in Aluminas" [Chantong and Massoth[11], Lee et al.[12]]. The prevailing explanation for restricted diffusion involves steric hindrance and hydrodynamical drag effects. Two recent papers on the diffusion of light gases in alumina have been published by Hou et al.[13] and Dugan and Dogu[14]. Hou et al.[13] reported that their experimental results demonstrated that diffusion occurs mainly in the bulk region up to 10 bars for the gases measured, and contrary to the usual predictions, the inverse proportionality of the effective diffusivity to the first

power of the pressure is not always obeyed. Dugan and Dogu[14] report variations in tortuosity values ranging from 1.77 to 2.78 for different tracers for alumina [mean pore radius, 280 Å and from 2.98 to 6.94 for Pd-alumina for the same tracers [mean pore radius, 800 Å]. Some of this difference was attributed to diffusion into dead-end pores for nonisobaric experiments. Adsorption of hydrogen was observed on the Pd-alumina in the Dugan and Dogu study. The largest molecule used in both these studies was CO_2.

In this study we measured the diffusivity of 1,3 di-isopropyl benzene and 1,3,5 tri-isopropyl benzene in NaY zeolite crystal, in alumina matrix particles and in FCC catalyst pellet (0.9 micron NaY zeolite) by ZLC method. The objective is to determine the mechanism of the diffusivity for the various systems to identify the controlling mechanism of mass transfer in the FCC catalyst pellet.

Theory

The diffusivities were measured using the ZLC technique [Eic and Ruthven[15]]. For the microporous zeolites, the calculated diffusivities were extracted from the long time solution of the standard equations using both the linear and nonlinear equations [Eic and Ruthven[15], Brandani[16]].

For macropore diffusion, the equivalent form of the expression was used with the effective diffusivity expressed as $D_{eff} = \dfrac{\varepsilon_P D_P}{\varepsilon_P + (1-\varepsilon_P)K}$ with D_P determined from $\dfrac{1}{D_P} = \tau_P\left(\dfrac{1}{D_m} + \dfrac{1}{D_k}\right)$. However, the alumina particles had a log-normal size distribution. For particles with a size distribution, the Laplace domain solution technique of Duncan and Moeller[17] was tried unsuccessfully. From an examination of the papers of Ruthven and Loughlin[18] and Duncan and Moller[17], it was decided to fit the experimental data for the size distribution in the region $0.2 \langle \left(1 - \dfrac{m_t}{m_\infty}\right) \rangle 0.08$ by solving numerically the normalized linear ZLC model at the mean particle diameter R_m. The assumption is that this gives a reasonable representative value of the diffusion coefficient. Also, as no analysis appears to have been made for the nonlinear asymptotic solution for a crystal size distribution for the ZLC, the value of the diffusivity calculated by the above procedure is assumed to not vary significantly from the value that the nonlinear asymptotic solution gives as is true for the linear case [Brandani[16]].

The FCC catalysts results were solved by applying the standard macropore solution to the entire curve and by using the long time solution. In the entire solution technique, the value of K used in the D_{eff} equation above is $K_{overall}$. For a linear system, $K_{overall} = [\omega K_z + (1-\omega)K_a]$ where ω is the mass fraction of zeolite in the catalyst and K_z and K_a are the equilibrium constants in the zeolite and alumina respectively. Unfortunately, the system is strongly nonlinear.

Results and Discussion:

A line diagram of the apparatus used is illustrated in Figure 1. The reproducibility of the apparatus and experimental procedure is reported elsewhere in a study on xylenes diffusion in H-ZSM5 zeolite and is excellent [Loughlin et al.[19]].

NaY Crystals

Details of the NaY catalyst used and properties of the hydrocarbons employed are supplied in Tables 1 and 2., Experimental values of measured diffusivities for both 1,3 di-isopropyl benzene [1,3 DIPB] and 1,3,5 triisopropyl benzene [1,3,5 TIPB] are tabulated in Table 3.calculated using the long time solution technique. The minimum kinetic diameters of 1,3 DIPB and 1,3,5 TIPB are 8.4 and 9.3 Å respectively, larger than the pore opening of 7.4 Å of the NaY zeolite. Desorption plots are shown in Figures 2 to 4. Apparent values of L and K, calculated from the long time equation are also reported. Apparent L value ranges from 4.46 to 6.23 and apparent K value ranges from 31,939 to 249,119 for 1,3 DIPB. As these are in the nonlinear range, the nonlinear long time solution technique was used to calculate the diffusivities and these are the values reported. Diffusivity values are in the range of 10^{-17} m^2/sec for 1,3 DIPB. Moore and Katzer[2] reported diffusivity value at 25 °C of around $2x10^{-17}$ m^2/sec, which is higher than our experimental results.. Mesitylene has same kinetic diameter as 1,3 DIPB, and diffusivity values are reported by Ruthven and Kaul[5]. Extrapolating their diffusivity values, we find that mesitylene has lower diffusivity values than

1,3 diisopropyl benzene. Mesitylene has three methyl group at 1,3,5 position and thus have less rotational flexibility. But 1,3 diisopropyl benzene may rotate and deform its structure to diffuse more easily through the pores and thus may has higher diffusivity values than mesitylene.

The diffusivity plots of 1,3,5 TIPB are presented in Figures 3 and 4. All the plots contained a discontinuity in the initial region of desorption. Figure 4 is an expanded view of this region, indicating probably two different diffusion regimes. Initially we have a slow desorption curve, which after some time (approximately 50 sec) reaches a percolation threshold, and becomes more rapid. A possible explanation of this phenomenon follows. The first hypothesis is that 1,3,5 tri-isopropyl benzene is not at all successful in penetrating inside the zeolite pores. It just adsorbs on the surface of zeolite, only 3% of the total area available, as most of the adsorbed area is inside the zeolite pores. But this would give a much faster desorption initially which is contrary to what is observed. The second postulate is that reaction occurs in the catalytic adsorbent. Initially we have a desorption curve which is controlled by the slow diffusion rate of unreacted 1,3,5 tri-isopropyl benzene. The unreacted material is postulated to occupy the outer shell of the crystal. In the interior of the crystal, all the 1,3,5 tri-isopropyl benzene is believed to have reacted to produce isomers of di isopropyl benzene and propylene, and it is postulated that there is no more unreacted material in the central core. As soon as the ZLC is switched to desorption, the desorption rate is controlled by the outer shell where the majority of the unreacted 1,3,5 tri-isopropyl benzene resides. In this outer shell three phenomena are presumed to occur simultaneously. These are 1) diffusion of 1,3,5 tri-isopropyl benzene out of the crystal, 2) diffusion of 1,3,5 tri-isopropyl benzene into the crystal interior from the outer shell due to the existence of a concentration gradient as the central core lacks any of this material due to reaction, and 3) reaction of 1,3,5 tri-isopropyl benzene to produce isomers of di isopropyl benzene and propylene The diffusivity in the first 50 seconds is then probably controlled by the diffusion of 1,3,5 tri-isopropyl benzene even if there are other molecules diffusing through the outer shell as the diffusion rates of these other molecules are controlled by the presence of a larger slower moving species. Thereafter when the majority of the 1,3,5 tri isopropylbenzene has reacted in the outer shell, the diffusion reaches a percolation threshold as the diffusing molecules will be the product of reaction which are the isomers of di isopropyl benzene and propylene. We will have co-diffusion of these two molecules out of the crystal probably in the nonlinear region. $D_{app,}$ then is a contribution of both driving forces.. This is what is reported in this study as the intrinsic parameters are not known. The reported diffusivity values of the long time nonlinear asymptotic solution of the ZLC model for 1,3,5 tri-isopropyl benzene thus appear to be for the co-diffusion of isomers of di isopropyl benzene and propylene and are expected to be greater than the single component diffusivity of 1,3 di-isopropyl diffusivity on its own.

It is not possible to estimate the diffusivity at the initial time region for two reasons at present. One, this is the region which is controlled by the time constant of the apparatus due to dead volume limitations, etc. A second reason is that the system is highly nonlinear, and the nonlinear solution parameter λ concerning the equilibrium loading is unknown, so that we cannot apply the nonlinear model of Brandani (1998). Further as it is probably a mixture of hydrocarbons, it will be difficult to calculate at any time. We solved the linear ZLC model using orthogonal collocation in this region, and found the diffusivities to be a factor of 3 to 6 times lower than for the asymptotic nonlinear solution but the values of L obtained were complex. It was the latter result that directed us to the nonlinear aspects of the solution.

A discontinuity somewhat similar in effect to the one reported here has been observed by Brandani et al.[20] while studying the countercurrent diffusion in a ZLC (CCZLC) apparatus of p-xylene (desorbing, smaller molecule) and o-xylene (adsorbing, larger kinetic diameter molecule) in large silicalite crystals. The question arises as to when does the percolation threshold occur in this work. Ruthven[21] in a study of diffusion in 4A and 5A zeolite, found that the system reached a percolation threshold when about 33% of the sodium ions were replaced by calcium ions. At that stage, the 4A structure had opened up sufficiently for the system to behave like a 5A zeolite, with sufficient passages available for the larger molecules to transit as if through a 5A zeolite. Using this analogy, it is postulated that when the concentration of 1,3,5 tri isopropylbenzene reaches 66.6% in the outer shell, sufficient passages are available for the di isopropylbenzene isomers to exit as if the 1,3,5 tri isopropylbenzene is no longer limiting the diffusivity.
We report the diffusivities at long time and for zero loading condition for 1,3,5 tri-isopropyl benzene but as mentioned above, the reported diffusivity values of the long time nonlinear asymptotic solution of the ZLC model for this material appear to be for the co-diffusion of isomers of di isopropyl benzene and propylene.

Using the linear ZLC model, apparent L values ranges from 3.69 to 14.14, satisfactory for kinetic measurements, and apparent K values ranging from 22,627 to 595,142 were calculated. As these are in the nonlinear range, the nonlinear long time technique was used to calculate the diffusivities and these are the values reported. The diffusivity values reported from the experiment are in the range of 10^{-16} -10^{-18} m^2/sec. The fit of the nonlinear straight line asymptotic solution and the linear ZLC using the parameters in Table 3 is shown on the Figures 2 and 3. The apparent activation energies for both 1,3 DIPB and 1,3,5 TIPB are included in Table 3.

Alumina Matrix

A scanning electron microscope picture of the alumina particles [Figure 5] revealed the presence of a size distribution of particles. These were plotted in a histograms for both a normal and log normal distribution [Figure 6] and the mean R_m determined {Table 4].As mentioned above, the experimental data were fitted for this size distribution in the region $0.02 \langle \left(1-\frac{m_t}{m_\infty}\right) \rangle 0.08$. by solving numerically the normalized linear ZLC model at the mean particle diameter $R_{m.}$ This is the elbow of the log-linear desorption curve and appears somewhat invariant with size distribution. Also, as no analysis appears to have been made for the nonlinear asymptotic solution for a crystal size distribution for the ZLC, the value of the diffusivity calculated by the above procedure is assumed to not vary significantly from the value that the nonlinear asymptotic solution gives as is true for the linear case [Brandani[16]].

ZLC desorption curves and theoretical fits for 1,3 DIPB and 1,3,5 TIPB are shown in Figure 7 and 8 and the results are tabulated in Tables 5and 6. For 1,3 DIPB, diffusivity value ranges from 1.08E-11 m^2/sec to 3.5E-11 m^2/sec, and K values from 38,200 to 84,900 and for 1,3,5 tri-isopropyl benzene, diffusivity value ranges from 2.36E-13 m^2/sec to 1.26E-12 m^2/sec, and K values from 181,000 to 792,000 which of course are highly nonlinear. Strong temperature dependency is observed in both cases. It should be noticed in all plots that the tail end the desorption curve tends to be curved due to the effect of crystal size distribution.

Calculations of the ratio D_{exp}/D_{th} for 1,3 DIPB and 1,3,5 TIPB are shown in the last column, with D_{th} calculated assuming macropore control. The theoretical diffusivity for a homogeneous particle for linear equilibrium is given by $D_{th}=\frac{\varepsilon_P D_P}{\varepsilon_P+(1-\varepsilon_P)K}$ where $\frac{1}{D_P}=\tau_P\left(\frac{1}{D_m}+\frac{1}{D_k}\right)$ and ε_P is the particle voidage, D_P is the pore diffusivity, K is the equilibrium constant, D_m is the molecular diffusivity, D_k is the Knudsen diffusivity, and τ_P is the particle tortuosity

The ratio is excellent for 1,3,5 TIPB but out by a factor of 14 for 1,3 DIPB. The latter result is attributed to the rapidity of the sorption of 1.3 DIPB in the alumina particles due to the small particle size, indicating that these measurements may be controlled by the time constant of the apparatus. From the results for 1,3,5 TIPB it is apparent that adsorption in alumina is macropore controlled.

FCC Catalyst particles

The properties of the FCC catalyst are given in Table 7 and the pore network is presented in Figure 9. This is a complex systems consisting of an 80% alumina macropore/mesopore matrix and 20 % NaY microporous zeolite both of which adsorb hydrocarbons. The analysis above has shown the NaY zeolite to be micropore controlled and the alumina to be macropore controlled. Desorption curves are shown in Figures 10 and 11 together with the desorption curves for the NaY crystals.

In the earlier analysis on the diffusivity of 1,3,5 tri-isopropyl benzene in NaY crystals, a kink was observed on the desorption curve and the reported measured desorption diffusivity was hypothesized to be the diffusivity of reacted products1,3 di-isopropyl benzene and propylene. Accordingly, it is anticipated that the diffusivity from the NaY crystals in the FCC pellets will be primarily by diffusion of these two products. However, the pellets consist of 80% alumina matrix, in which the diffusion of unreacted 1,3,5 tri-isopropyl benzene is expected to occur. Accordingly exiting the pellet initially will be three species, 1,3,5 tri-isopropyl benzene, 1,2 di-isopropyl benzene and propylene. With the passage of time, the exodus of

1,3,5 tri-iso-propyl benzene will finish earlier than the exodus of 1,3 di-iso propyl benzene and propylene. In effect in the later stages of the desorption cycle, all that is being measured is the diffusivity of these two compounds from the zeolite matrix. As the long time solution of the ZLC technique is only relevant to the last stages of the desorption cycle, the diffusivity of the material measured is basically that of the co-diffusion of di-isopropyl isomers and propylene. In the paragraph that follows, when we speak of the diffusivity of 1,3,5 tri-iso propyl benzene in the long time region, it is really the co-diffusion of these two species that is occurring.

The data was analyzed using the long time solution of standard ZLC diffusion linear and nonlinear equations. A more appropriate model would have been analogous to the Silva and Rodrigues (1996) model, to account for macropore and micropore (crystal) diffusivity in the ZLC. The general pellet equation used by these authors was $\varepsilon_p \frac{\partial C_p}{\partial t} + (1+\varepsilon_p)\frac{\partial \overline{C_s}}{\partial t} = \varepsilon_p D_p \frac{1}{R^2}\frac{\partial}{\partial R}\left(R^2 \frac{\partial C_p}{\partial R}\right)$ but in this study, there is adsorption on both alumina and zeolite which is not accounted for in this model. The equilibrium constant ($K_{Overall}$) values vary from $1.1x10^4$ to $9.8x10^4$, indicating nonlinearity region. Apparent theoretical macropore diffusivities are in the range of $5x10^{-11}$ to $5x10^{-12}$ m^2/sec, whereas experimental values lie between $6.11x10^{-13}$ to $5.14x10^{-14}$ m^2/sec. This suggests macropore diffusion is not the controlling resistance in the long term region. In fact, the diffusivities are comparable to the NaY zeolite as the long time slopes are identical. They are displaced due to significant adsorption on the alumina. Further although, the long time solution is similar to that for NaY zeolite, the short to intermediate time solution is not on the long time solution curve, In this region, which occurs rapidly, and represents about 90 % of the mass adsorbed the desorption may be macropore controlled. A total analysis of this system is difficult due to the unavailability of the isotherms.

One of the ways to determine whether the system is macropore or micropore controlled is by comparing the diffusivity data for both crystal and pellet system. For a micropore control system pellet must have the same diffusivity values as in crystals, for the same crystal particle size. For 1,3 di-isopropyl and 1,3,5 tri-isopropyl benzene both pellet and crystal desorption curves have same slope in the long time region, which suggest they have same diffusion time constant. For pellets there is a rapid drop of concentration initially. This is due to desorption of the hydrocarbons from the alumina matrix macropores which depletes faster than the zeolite at the start of desorption. Later on when the alumina matrix is nearly depleted, the sorbate mainly exits from the crystal pores. Simulations have been undertaken taking the crystal diffusivity value as the diffusivity and the appropriate L value for pellet system. The figures are presented in Figure 10 and 11. Simulation line fits the long time pellet data perfectly; hence for 1,3 di and 1,3,5 tri-isopropyl benzene, the crystal and pellet have the same diffusion time constant and are micropore controlled system in the long time region.

Arrhenius plot for 1,3 di-isopropyl benzene and 1,3,5 tri-isopropyl benzene are indicated in Figure 12. Diffusional time constant is plotted against 1000/T. It is clear that for both systems, crystal and pellet diffusional time constant values are close to each other. The activation energy for 1,3 di-isopropyl benzene is 66 kJ/mol and 1,3,5 tri-isopropyl benzene is 77.35 kJ/mol.

Conclusions

The diffusivities of 1,3 di-isopropyl benzene and 1,3,5 tri-isopropyl benzene on NaY zeolite, alumina particles and FCC catalysts have been measured. On NaY crystals, the diffusivities are micropore controlled, with 1,3,5 tri –isopropyl benzene having a percolation threshold, indicating possible cracking. The alumina particles with varying size distribution were macropore controlled. The FCC catalysts diffusivities reported are micropore controlled in the long time region. However, the short time region is probably macropore controlled.

References

(1) Satterfield, C.N., and Katzer, J.R. Counterdiffusion of Liquid Hydrocarbons in Type Y Zeolites. Adv. Chem. Ser., 1971, 193-208.

(2) Moore, R. M., Katzer, J. R. Counter diffusion of liquid hydrocarbons in type Y zeolite. Effect of molecular size, molecular type and diffusion direction. AIChE J., 1972 18, 876.

(3) Moore, R. M. Counter diffusion of Liquid Hydrocarbons in the type Y Zeolite. Effect of Molecular Size, Shape and Type. Chem. Eng. J., 1971, 6, 38-42.
(4) Culfaz, A., Ergun, G. Counterdiffusion of liquid hydrocarbon pairs in ion-exchanged forms of zeolite X. Sep. Sci. and Tech., 1986, 21(5), 495-517.
(5) Ruthven, D. M., Kaul B. K. Adsorption of aromatic hydrocarbons in NaX zeolite. 2. Kinetics. Ind. Eng. Chem. Res.,1993, 32, 2053-2057.
(6) Fujikata, Y, Masuda, T., Ikeda, H., Hasimoto, K. Measurment of the diffusivities with MIF and Y type zeolite catalysts in adsorption and desorption processes. Microporous and Mesoporous Materials, 1998, 21(4-6), 679-686.
(7) Hashmoto, S., Hagiri, M., Barzykin, A. V. Triplet-Triplet Energy Transfer as a Tool for Probing Molecular Diffusivity within Zeolites. J. Phys. Chem. B, 2002, 106(4), 844-852.
(8) Cavalcante, C. L. Jr., Silva, N. M., Souza, E. F., Sobrinho, E. V. Diffusion of paraffins in dealuminated Y mesoporous molecular sieve. Adsorption, ,2003, 9, 205-212.
(9) S-Aguiar, E. F., Murta-Valle, M. L., Cardoso, D., Cracking of 1,3,5-triisopropylbenzene over deeply dealuminated Y zeolite. Studies in Surface Science and Catalysis Zeolites: A Refined Tool for Designing Catalytic Sites, 1995, 97, 417-422.
(10) Al-Khattaf, S., Atias, A. J., de Lasa, H. I., Diffusion and Catalytic Cracking of 1,3,5 tri-isopropyl benzene in FCC Catalysis. Chem. Eng. Sci., 2000c, 57(22-23), 4909-4920.
(11) Chantong, A.; Massoth, F. E., Restrictive diffusion in aluminas**,** AIChE J, (1983), 29(5), 725-31.
(12) Lee, S. Y.; Seader, J. D.; Tsai, Chung H.; Massoth, F. E., Restrictive liquid-phase diffusion and reaction in bidisperse catalysts, Industrial & Engineering Chemistry Research (1991), 30(8), 1683-93.
(13) Hou, K.; Fowles, M.; Hughes, R., Effective diffusivity measurements on porous catalyst pellets at elevated temperature and pressure, Chem. Eng. Res. and Des., (1999), 77(A1), 55-61.
(14) Dogan, Meltem; Dogu, Guelsen., Dynamics of flow and diffusion of adsorbing gases in Al_2O_3 and Pd-Al_2O_3 pellets., AIChE Journal (2003), 49(12), 3188-3198
(15) Eic, M., Ruthven, D. M. A New Experimental Technique for Measurement for Intracrystalline Diffusivity. Zeolites, 1988, 8, 40-45.
(16) Brandani, S., Effects of Nonlinear Equilibrium on Zero Length Column Experiments, Chem. Eng. Sci., 1998, 53(15), 2719-2798.
(17) Duncan, W. L.; Moller, K. P.; "The Effect of a Crystal Size Distribution on ZLC Experiments"; Chemical Engineering Science, 57(14): 2641-2652 (2002)
(18) Ruthven, D. M., Loughlin, K. F., "Effect of crystal size distribution on diffusion measurements in molecular sieves", Chem. Eng. Sci. 26(5), 577-84 (1971
(19) Loughlin, Kevin F., Zaman, Sharif F. and Al-Khattaf, Sulaiman A., Investigation of Diffusivities of Xylene Isomers in ZSM-5 Zeolite by Zero Length Column Method, Submitted to Adsorption Journal, 2004.
(20) Brandani, S; Jama, M. A.; Ruthven, D. M.; "Diffusion, Self Diffusion and Counterdiffusion of Benzene and p-Xylene in Silicalite", Microporous and Mesoporous Material, 35-6: 283-300; (2000a).
(21) Ruthven, D. M. Diffusion in Partially Ion Exchanged Molecular Sieves. Canadian Journal of Chemistry, 1974, 52 (20), 3523-3528

ACKNOWLEDGMENTS
The authors wish to acknowledge the support of King Fahd University of Petroleum & Minerals (Project SABIC/2003-13) during the course of this work and preparation of this paper.

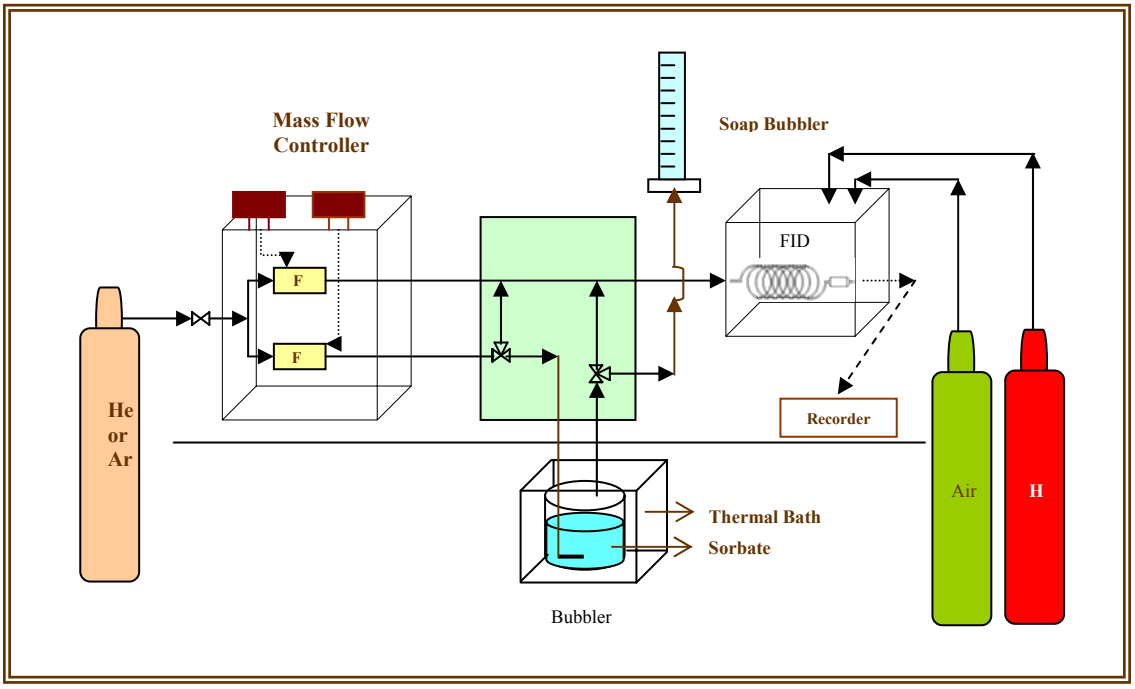

Figure 1: Schematic Diagram of experimental setup

Table 1: Properties of Y catalyst

Zeolite Type	Faujasite	SiO_2/Al_2O_3 (mole/mole)	5.7	Na_2O (wt. %)	0.25
Pore size(Å)	7.4	Unit cell size (Å)	24.51	Crystal size (μm)	0.9

Table 2: Properties of Hydrocarbons

Hydrocarbon Name	Chemical Formula	Molecular weight	Boiling point (^oC)	Partial Pressure (psi)	Molecular size-Min Kinetic (Å)
1,3 di isopropyl benzene	$C_{12}H_{18}$	162.28	210	5.75e-4	8.4
1,3,5 tri isopropyl benzene	$C_{15}H_{24}$	204.36	233	5.0989e-5	9.3

N.B. : Boiling Points and Vapor Pressure are taken from HYSYS software database.

Table 3 Diffusivity values for the Hydrocarbon molecules in NaY Zeolite:

Hydrocarbon	Temperature (^oC)	D/R^2 (sec^{-1})	D (m^2/sec)	D^* (m^2/sec)	E (kJ/mol)	L	K
Data results for 1,3 Di-Isopropyl Benzene in Y zeolite							
1,3 DIPB	150	8.35E-05	1.69E-17	3.00E-09	66.14	6.23	249119.56
	170	2.06E-04	4.17E-17			4.61	136287.37
	190	3.87E-04	7.84E-17			4.88	68501.17
	210	9.08E-04	1.84E-16			4.46	31939.09
Data results for 1,3,5 Tri-Isopropyl Benzene in Y zeolite							
1,3,5 TIPB	125	1.74E-05	3.53E-18	1.00E-07	77.74	14.14	595142.80
	150	8.35E-05	1.69E-17			6.56	286552.25
	170	3.14E-04	6.35E-17			5.47	91579.29
	190	1.13E-03	2.30E-16			3.69	22627.97
	75	4.87E-05	9.87E-18			8.81	x
	125	7.75E-05	1.57E-17			10.2	x
	150	4.46E-04	9.04E-17			3.56	x

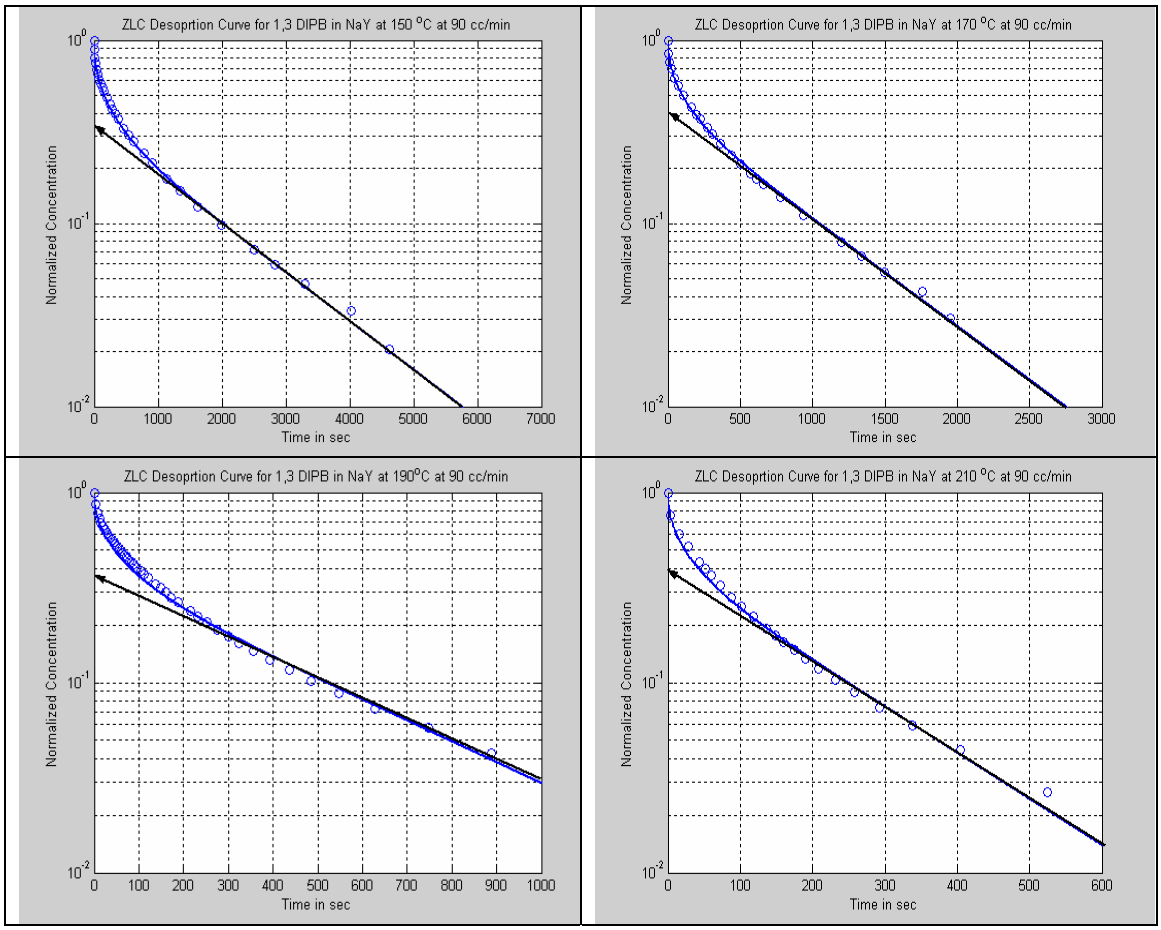

Figure 2: ZLC desorption curve for 1,3 di-Isopropyl benzene at 90 cc/min for temperature range 150-210 ^{o}C

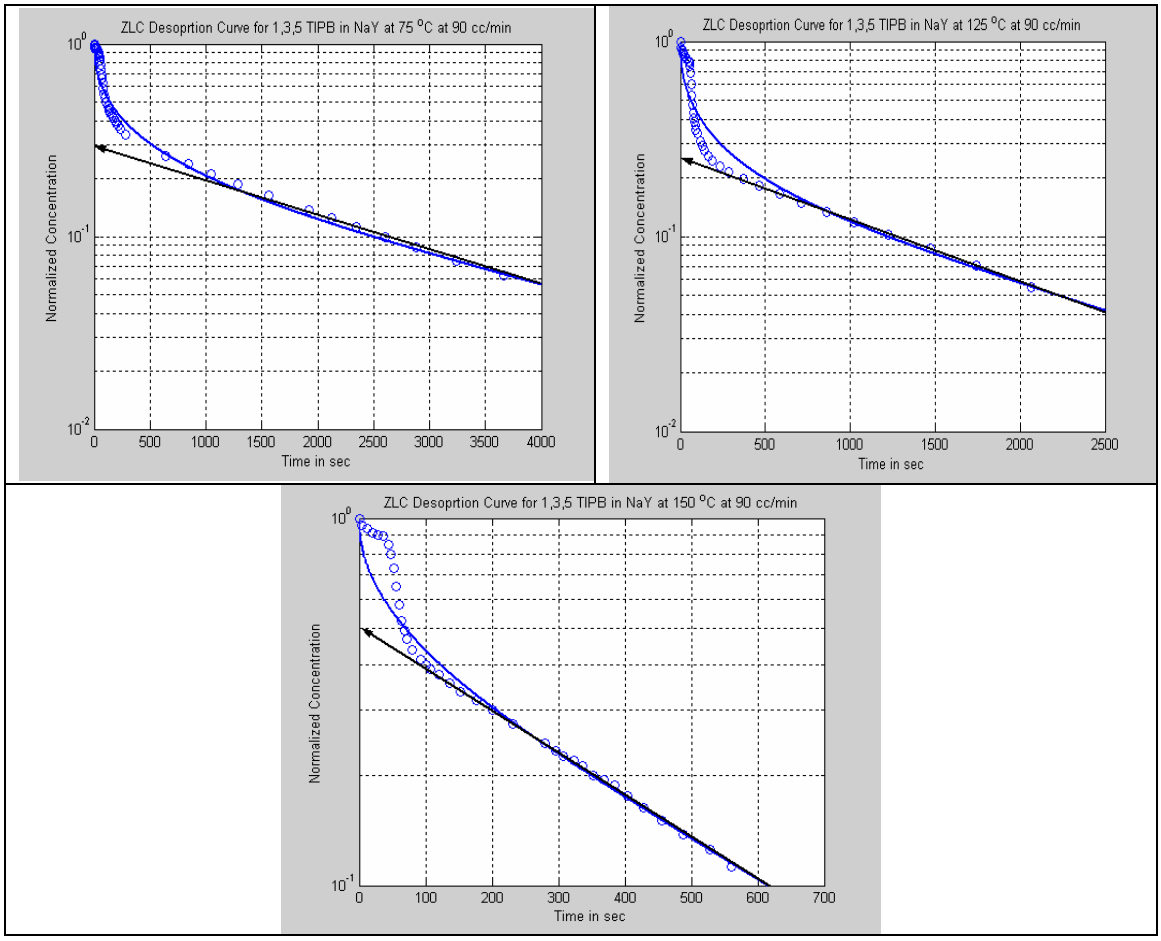

Figure 3: ZLC desorption curve for 1,3,5 tri-Isopropyl benzene at 90 cc/min for temperature range 75-125 ^{o}C

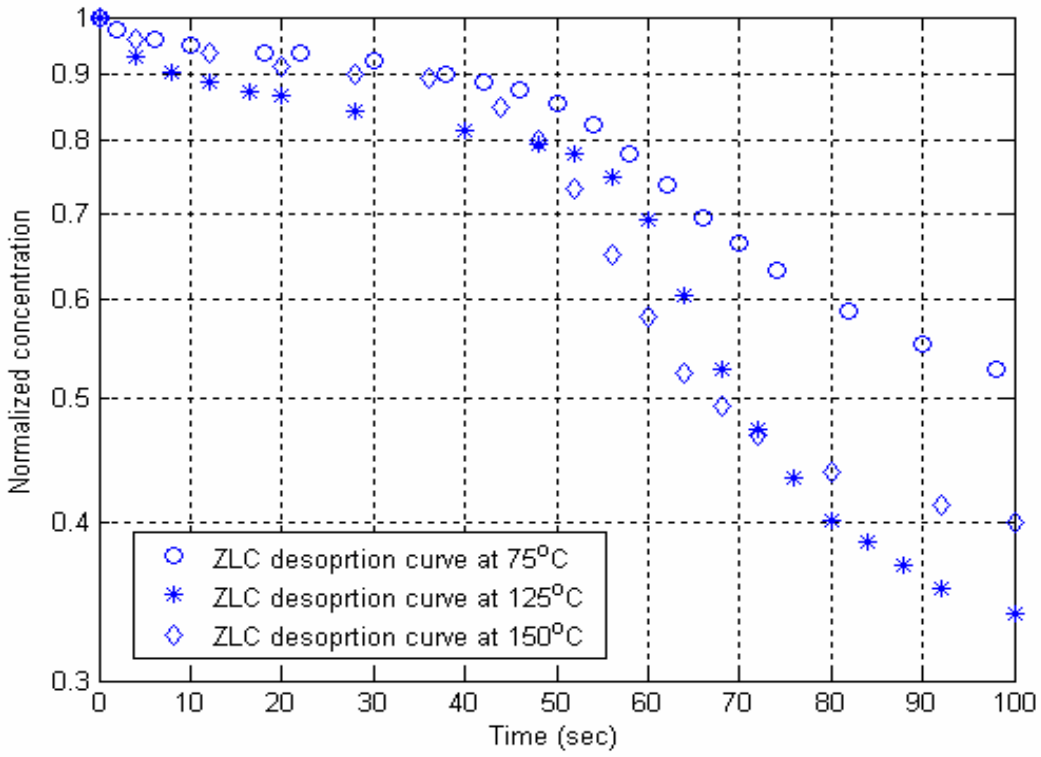

Figure 4. Expanded view of the initial region of the desorption curve for 1,3,5 tri-isopropylbenzene. The flowrate is 90 cc/min.

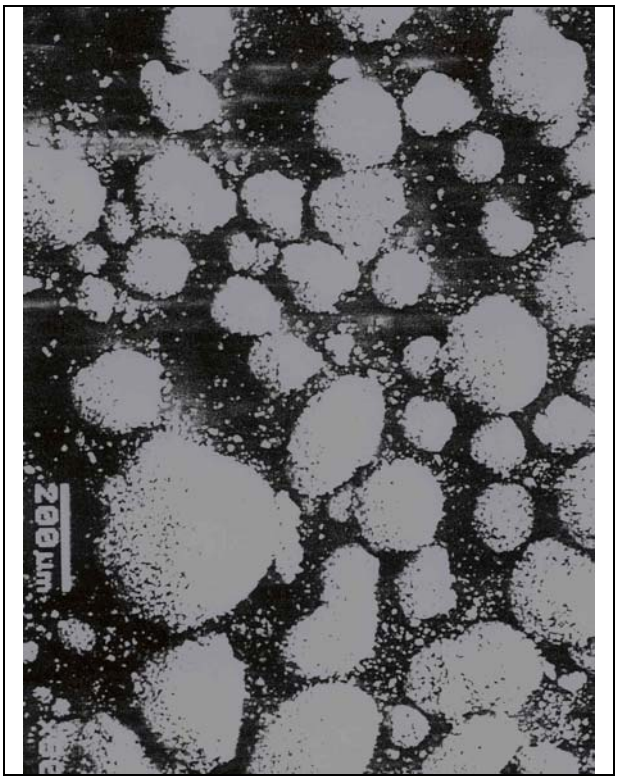

Figure 5: SEM analysis of alumina crystal

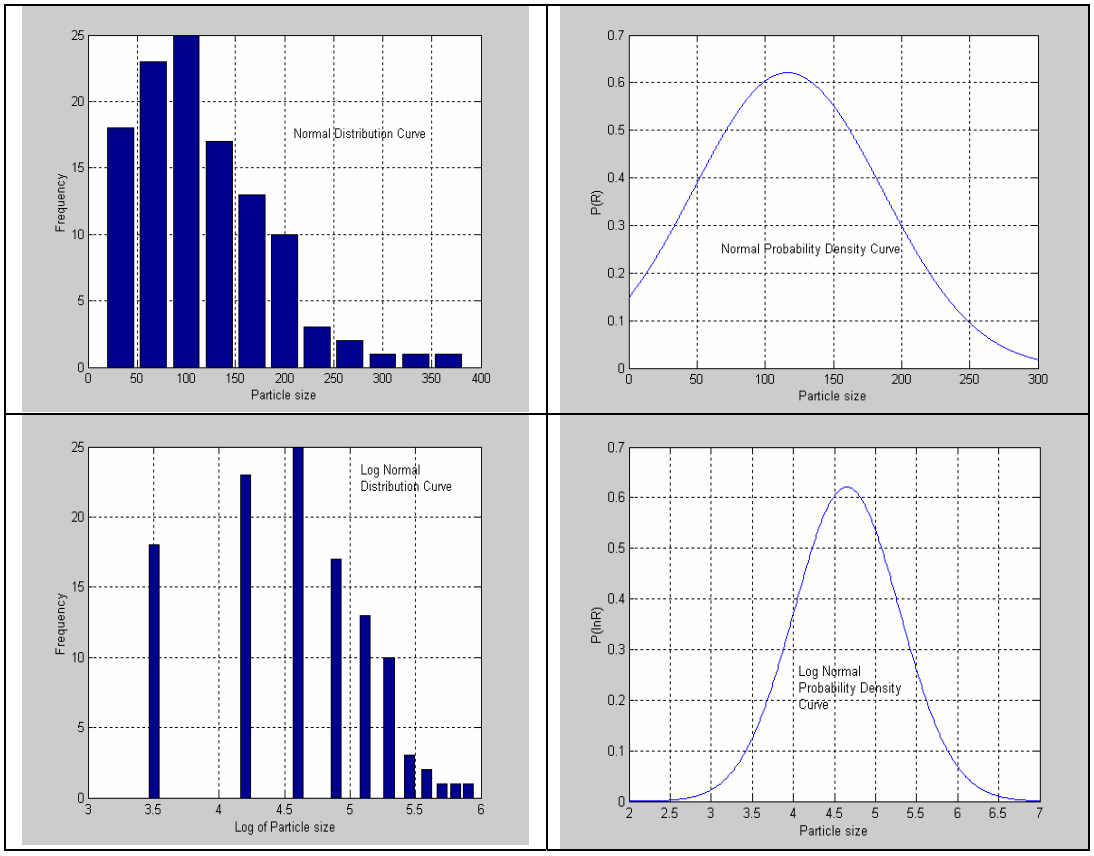

Figure 6: Particle size distribution curve for alumina crystal

Table 4: Statistical analysis for particle size distribution of alumina crystal

	Normal Distribution	Log Normal Distribution
Mean diameter (μm)	116.667	4.65
Standard deviation (σ)	68.95	0.64
Skewness (SK)	0.72	0.22
Goodness of fit	2.94	2.7

Table 5: Numerical Calculation of effective diffusivity of 1,3 di-isopropyl benzene in alumina particles.

Temp (^oC)	Molecular Diffusivity D_{ab} (cm^2/sec)	Knudsen Diffusivity D_{ka} (cm^2/sec)	Pore Diffusivity D_p (cm^2/sec)	Equilibrium Constant (K)	Effective Diffusivity (m^2/s)	Experimental Diffusivity (m2/s)	Ratio D_{exp}/D_{th}
150	1.25E-01	3.92E-02	4.97E-03	8.49E+04	3.15E-12	1.42E-11	12.80
170	1.36E-01	4.01E-02	5.16E-03	6.10E+04	4.55E-12	2.19E-11	13.79
190	1.47E-01	4.10E-02	5.34E-03	4.34E+04	6.63E-12	3.50E-11	15.32
210	1.58E-01	4.19E-02	5.52E-03	3.82E+04	7.77E-12	4.37E-11	16.47

Table 6: Numerical Calculation of effective diffusivity of 1,3,5 tri-isopropyl benzene in alumina crystal.

Temp (^oC)	Molecular Diffusivity D_{ab} (cm^2/sec)	Knudsen Diffusivity D_{Ka} (cm^2/sec)	Pore Diffusivity D_p (cm^2/sec)	Equilibrium Constant (K)	Effective Diffusivity (m^2/s)	Experimental Diffusivity (m^2/s)	Ratio D_{exp}/D_{th}
125	9.81E-02	3.39E-02	4.20E-03	7.92E+05	2.85E-13	9.58E-13	0.93
150	1.09E-01	3.49E-02	4.41E-03	4.22E+05	5.63E-13	1.88E-12	0.95
170	1.18E-01	3.57E-02	4.57E-03	2.08E+05	1.18E-12	3.96E-12	0.94
190	1.28E-01	3.65E-02	4.74E-03	1.81E+05	1.41E-12	5.13E-12	1.05

* Porosity = 0.35, Tortuosity = 3, Pressure = 3 atm., $MW_{1,3DIPB}$ = 162 gm/mol, $MW_{1,3,5\ TIPB}$ = 204 gm/mol, d_{pore} = 70 Å, R_m= Mean Radius, Particle Size Distribution

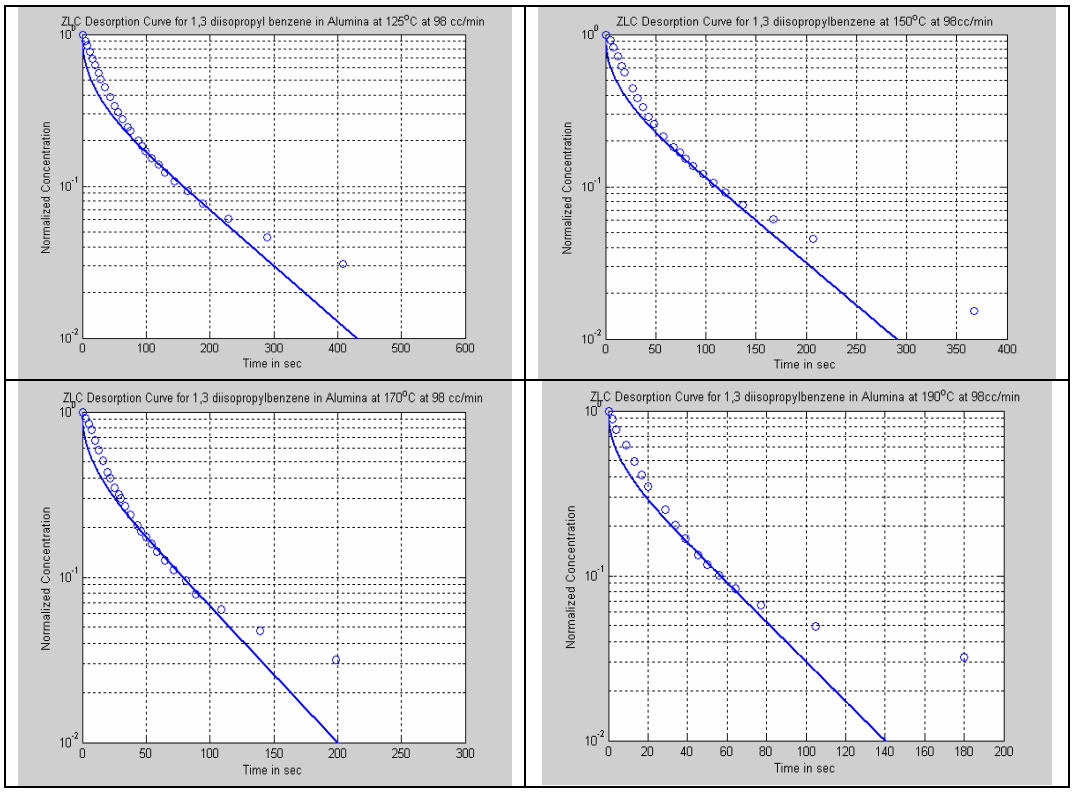

Figure 7: ZLC desorption curves for 1,3 di-isopropyl benzene in Alumina crystals at 98 cc/min

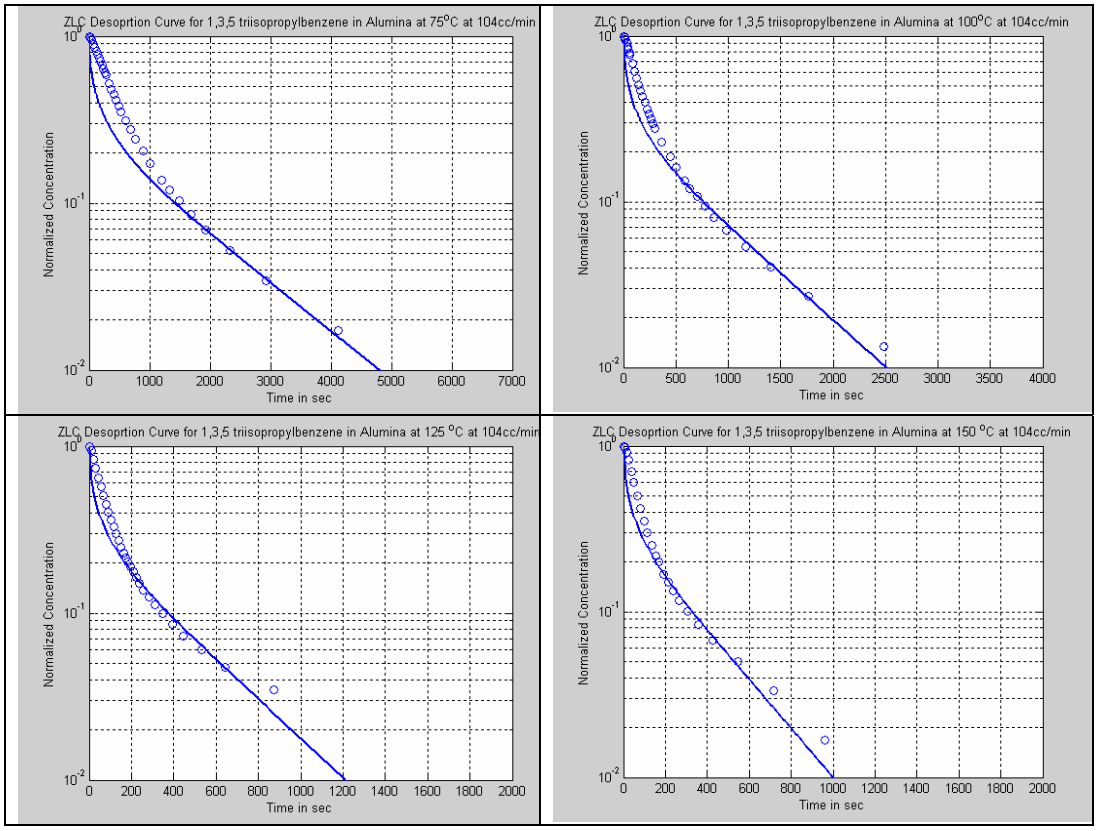

Figure 8: ZLC desorption curves for 1,3,5 tri-isopropyl benzene in Alumina crystals at 104 cc/min

Table 7: Properties of FCC catalyst

Pellet size (μm) *	50
Macropore size (Å) [1]	500
NaY Crystal size (μm) [1]	0.9
Hydrated pellet Density (gm/cc) [12]	1.5
Porosity [12]	0.5
Matrix [1]	SiO_2 (20 %) and Al_2O_3 (80 %)
Crystal vol (wt %) [1]	20

Ref : * SEM analysis, KFUPM-RI, 2003.

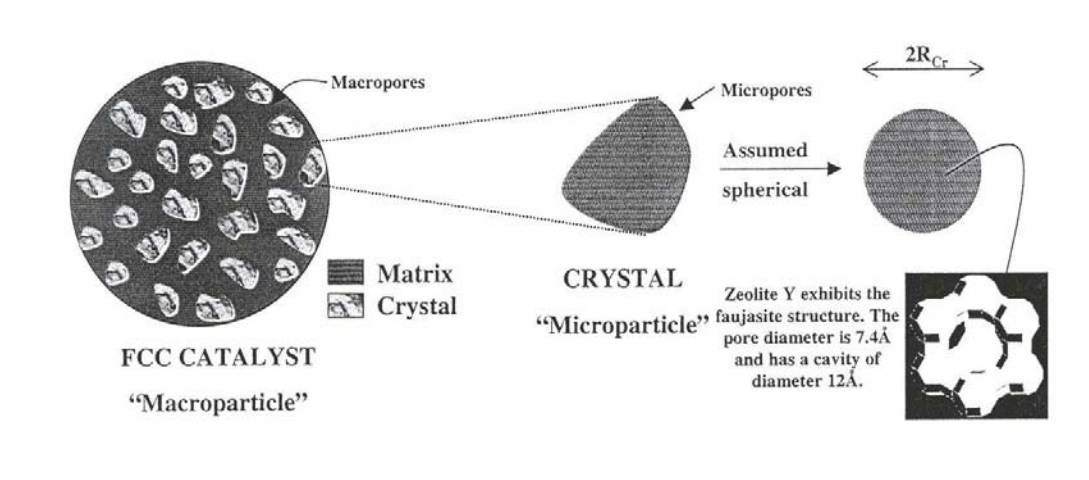

Figure 9: Pore network structure in a FCC pellet

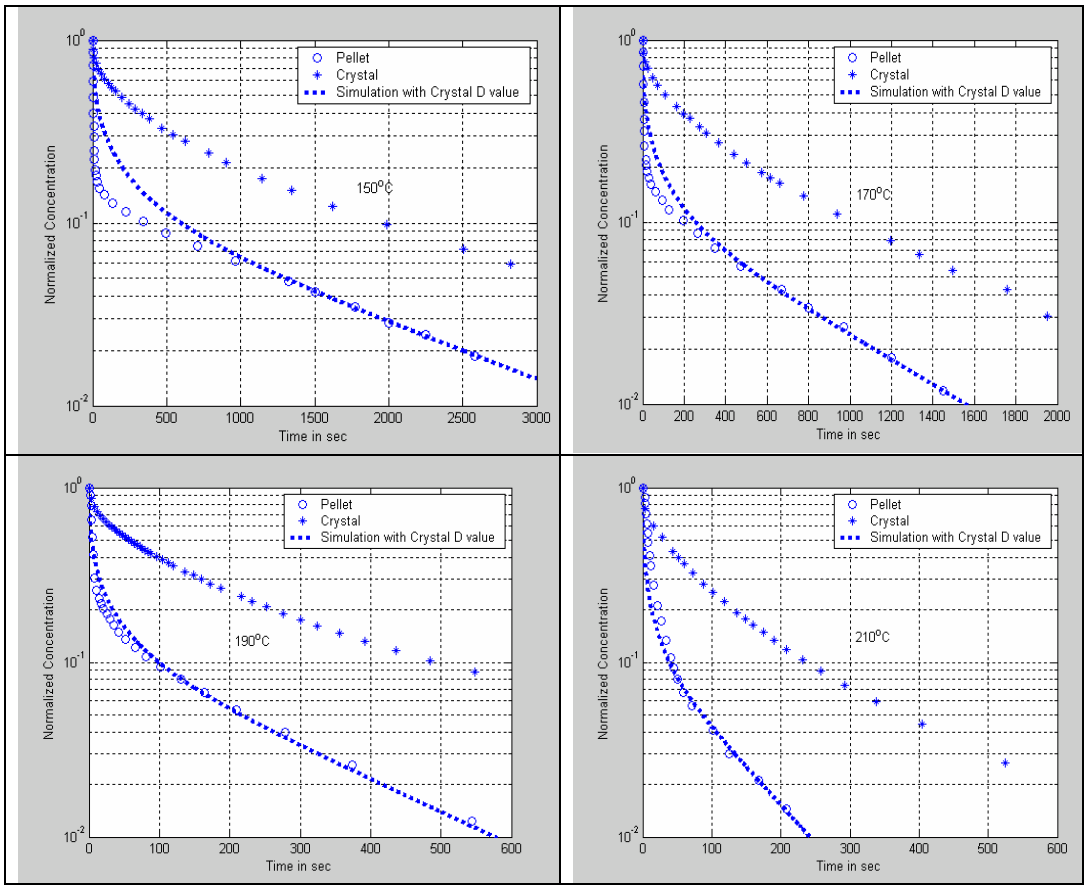

Figure 10: Comparison curve for pellet and crystal data for 1,3 di-isopropylbenzene

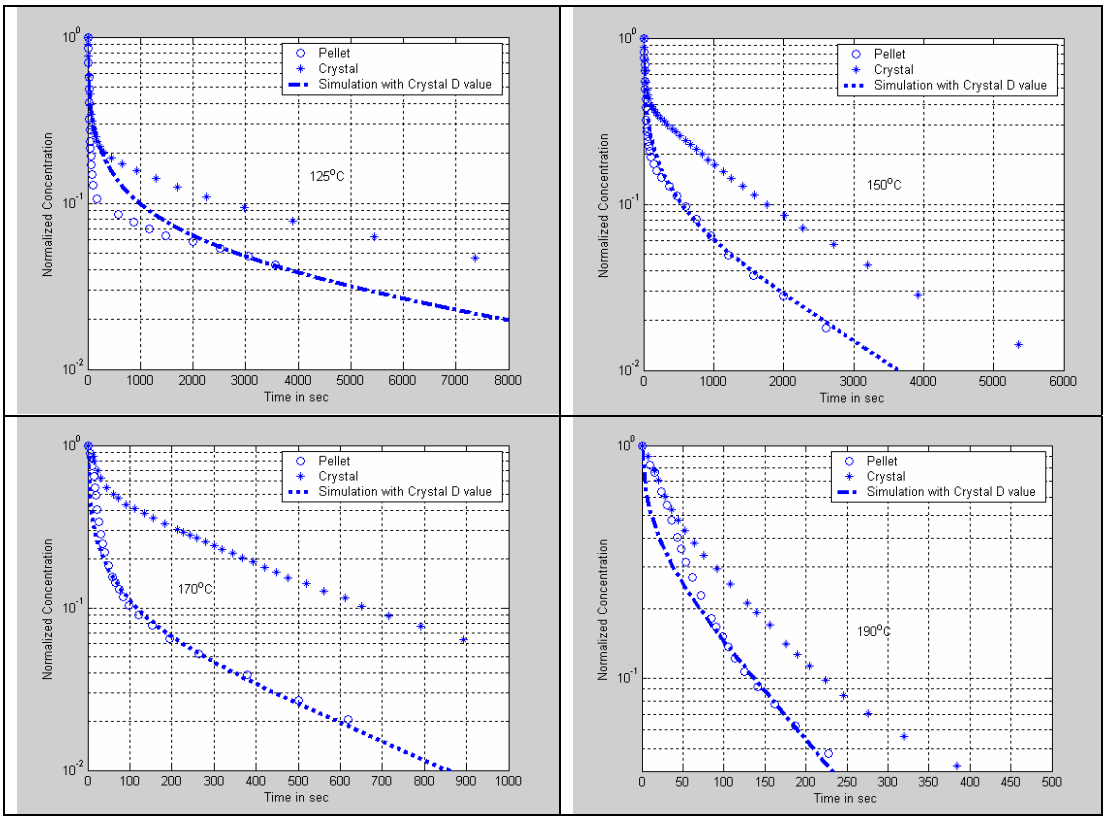

Figure 11: Comparison plot for pellet and crystal data for 1,3,5 tri-isopropyl benzene

Table 10: **Diffusivity of di-isopropyl benzene in FCC pellets (0.9 micron NaY Crystal), 50μm pellet diameter (55-45 μm pellet size distribution), purge gas velocity 90cc/min**.

Temperature (^oC)	1000/T	D_{ap}/R^2	Apparent diffusivity D_{ap} (m^2/sec)	Theoretical apparent diffusivity D_{ap} (m^2/sec)	L	$K_{overall}$
150	2.36	8.22E-05	5.14E-14	5.48E-12	25.61	9.08E+04
170	2.25	1.77E-04	1.11E-13	9.81E-12	20.51	5.26E+04
190	2.15	4.93E-04	3.08E-13	2.35E-11	17.09	2.27E+04
210	2.07	1.10E-03	6.88E-13	5.00E-11	15.76	1.10E+04

Table 11: Diffusivity of 1,3,5 tri-isopropyl benzene in FCC pellets (0.9 micron NaY Crystal), 50μm pellet diameter (55-45 μm pellet size distribution), purge gas velocity 94cc/min.

Temperature (^oC)	1000/T	D_{ap}/R^2	Apparent diffusivity D_{ap} (m^2/sec)	Theoretical apparent diffusivity D_{ap} (m^2/sec)	L	$K_{overall}$
125	2.51	1.33E-05	8.31E-15	2.80E-12	100	1.50E+05
150	2.36	7.17E-05	4.48E-14	2.71E-12	17.09	1.63E+05
170	2.25	2.90E-04	1.81E-13	2.26E-11	34.04	2.02E+04
190	2.15	1.40E-03	8.75E-13	1.71E-11	5.14	2.77E+04

Table 8: Diffusivity of di-isopropyl benzene in FCC pellet (0.9 micron NaY Crystal) 50μm pellet diameter (55-45 μm pellet size distribution) purge gas velocity 90cc/min.

Temperature (^oC)	1000/T	D_{ap}/R^2	Apparent diffusivity D_{ap} (m^2/sec)	Theoretical apparent diffusivity D_{ap} (m^2/sec)	L	$K_{overall}$
150	2.36	8.22E-05	5.14E-14	5.48E-12	25.61	9.08E+04
170	2.25	1.77E-04	1.11E-13	9.81E-12	20.51	5.26E+04
190	2.15	4.93E-04	3.08E-13	2.35E-11	17.09	2.27E+04
210	2.07	1.10E-03	6.88E-13	5.00E-11	15.76	1.10E+04

Table 9: Diffusivity of 1,3,5 tri-isopropyl benzene in FCC pellet (0.9 micron NaY Crystal) 50μm pellet diameter (55-45 μm pellet size distribution) purge gas velocity 94cc/min.

Temperature (^oC)	1000/T	D_{ap}/R^2	Apparent diffusivity D_{ap} (m^2/sec)	Theoretical apparent diffusivity D_{ap} (m^2/sec)	L	$K_{overall}$
125	2.51	1.33E-05	8.31E-15	2.80E-12	100	1.50E+05
150	2.36	7.17E-05	4.48E-14	2.71E-12	17.09	1.63E+05
170	2.25	2.90E-04	1.81E-13	2.26E-11	34.04	2.02E+04
190	2.15	1.40E-03	8.75E-13	1.71E-11	5.14	2.77E+04

Figure 12: Arrhenius plots of 1,3 di-isopropyl benzene and 1,3,5 tri-isopropyl benzene in both FCC pellets and NaY crystal